Local and Long-Range Reciprocal Regulation of cAMP and cGMP in Axon/Dendrite Formation

Maya Shelly, *et al.*

Science **327**, 547 (2010);
DOI: 10.1126/science.1179735

Local and Long-Range Reciprocal Regulation of cAMP and cGMP in Axon/Dendrite Formation

Maya Shelly,[1]* Byung Kook Lim,[1]* Laura Cancedda,[1,2] Sarah C. Heilshorn,[1]† Hongfeng Gao,[1] Mu-ming Poo[1]‡

Cytosolic cyclic adenosine monophosphate (cAMP) and cyclic guanosine monophosphate (cGMP) often mediate antagonistic cellular actions of extracellular factors, from the regulation of ion channels to cell volume control and axon guidance. We found that localized cAMP and cGMP activities in undifferentiated neurites of cultured hippocampal neurons promote and suppress axon formation, respectively, and exert opposite effects on dendrite formation. Fluorescence resonance energy transfer imaging showed that alterations of the amount of cAMP resulted in opposite changes in the amount of cGMP, and vice versa, through the activation of specific phosphodiesterases and protein kinases. Local elevation of cAMP in one neurite resulted in cAMP reduction in all other neurites of the same neuron. Thus, local and long-range reciprocal regulation of cAMP and cGMP together ensures coordinated development of one axon and multiple dendrites.

The polarization of postmitotic neurons involves the differentiation of a single axon and multiple dendrites. The process of neuronal polarization begins with the specification of the axon/dendrite identity of undifferentiated neurites, followed by selective localization of molecules that are responsible for differential growth and specific functions of the axon and dendrites (*1*, *2*). The initial axon/dendrite specification may result from cytoplasmic asymmetry caused by the last mitotic division of the neural progenitor cell (*3*), the stochastic fluctuation of cytoplasmic determinants (*1*, *2*, *4*, *5*), or the action of extracellular polarizing factors (*6*–*12*). In cultured hippocampal neurons, neuronal polarization appears to begin with selective accumulation/activation of key components into one undifferentiated neurite (*1*, *8*, *9*, *12*–*19*) that triggers its rapid growth and axon differentiation. To ensure the formation of one axon and multiple dendrites, axon initiation at one neurite must be accompanied by long-range signals that suppress axon formation or promote dendrite formation in other neurites. We investigated the role of two second messengers, cyclic adenosine monophosphate (cAMP) and cyclic guanosine monophosphate (cGMP), in mediating the coordinated differentiation of one axon and multiple dendrites.

Antagonistic axon/dendrite initiation by local cAMP/cGMP activity. Dissociated embryonic hippocampal neurons undergo spontaneous polarization on a uniform culture substratum, from a morphologically symmetric cell after plating to a polarized neuron exhibiting a single axon and multiple dendrites within a few days (*20*, *21*). First, we examined the effect of localized cAMP and cGMP activities in axon/dendrite initiation by plating these neurons on substrates coated with stripes of membrane-permeant fluorescent analogs of cAMP or cGMP [F-cAMP or F-cGMP; see supporting online material (SOM)]. The neurons were imaged at 12 hours after plating and were immunostained after further incubation of 48 hours with the axon marker Smi-312 and the somatodendritic marker MAP2. At 12 hours, cells exhibited several short neurites of similar lengths (Fig. 1, A and B). By 60 hours, axons were found on the F-cAMP stripe or off the F-cGMP stripe, whereas dendrites were mostly found off the F-cAMP stripe or on the F-cGMP stripe (Fig. 1, A and B). We analyzed the distribution of axon/dendrite initiation sites on the soma at 48 to 60 hours after plating, when neurons had completed the polarization process, for all polarized cells with the soma located at the stripe boundary (Fig. 1Ca). This retrospective analysis of axon/dendrite initiation was possible because neurite initiation sites on the soma did not move during neuronal polarization (Fig. 1, A and B). The distribution of the axon initiation site showed preference for initiation on the F-cAMP stripe and off the F-cGMP stripe, but no preference for stripes coated with bovine serum albumin (Fig. 1Cb). The distribution of dendrite initiation sites showed opposite preference (Fig. 1Cb). Analysis of the preference index {PI = [(% on stripe) – (% off stripe)]/100%} showed that localized cAMP and cGMP activities were sufficient to induce preferential initiation of axons and dendrites, respectively (Fig. 1D). These effects are distinct from the known effects of cAMP and cGMP on the guidance of growth cones (*22*, *23*) that were also revealed by the axon/dendrite pathfinding at the stripe boundary (Fig. 1, A and B).

Next, we plated these neurons on a substrate striped with either the adenylate cyclase (AC) inhibitor SQ-22536 or the protein kinase A (PKA) inhibitor KT5720 or Rp-8-Br-cAMPS, to reduce locally basal cAMP/PKA activity. For neurons with the soma located at the stripe boundary, axons were mostly initiated off the stripes (Fig. 1, Cb and D), similar to that found on the F-cGMP–striped substrate. Conversely, when the neurons were plated on a substrate striped with the soluble guanylate cyclase (sGC) inhibitor ODQ or the protein kinase G (PKG) inhibitor KT5823 or Rp-8-pCPT-cGMPS, axons were initiated mostly on the stripe (Fig. 1, Cb and D), similar to that found for F-cAMP stripes. There was also a preference for the dendrite to be initiated off the ODQ/KT5823/Rp-8-pCPT-cGMPS stripes, but on the SQ-22536/KT5720/Rp-8-Br-cAMPS stripes (Fig. 1, Cb and D). Thus, asymmetry in the basal cAMP or cGMP activity is sufficient to trigger axon/dendrite polarization, and cAMP and cGMP activities exert antagonistic actions on this process.

Reciprocal regulation between cAMP and cGMP. Antagonistic cellular actions mediated by cAMP and cGMP (*23*–*28*) could result from opposing actions of cAMP and cGMP pathways on common cellular targets. However, crosstalk between these two pathways could also occur by reciprocal regulation between cAMP and cGMP, as suggested by findings from non-neuronal systems (*28*, *29*). We used genetically encoded fluorescence resonance energy transfer (FRET) reporters to examine directly the reciprocal regulation between cAMP and cGMP in cultured hippocampal neurons. The neurons were transfected 2 hours after cell plating with a construct encoding one of the three FRET reporters: indicator of cAMP using Epac (ICUE) (*30*), cGMP energy transfer sensor derived from PDE5A (cGES-DE5) (*31*), or A-kinase activity reporter (AKAR) (*32*) (SOM text), which were designed to monitor the amount of cAMP, cGMP, and PKA activity, respectively. All FRET measurements were made 10 to 16 hours after cell plating, before axon/dendrite differentiation (*20*, *21*). Bath application of the membrane-permeant cAMP analog Sp-8-Br-cAMPS (20 μM) or the AC activator forskolin (20 μM) resulted in a global increase of cAMP and PKA signals in ICUE- and AKAR-expressing cells, respectively, as measured by the increase in the ratio of yellow fluorescent protein (YFP) to cyan fluorescent protein (CFP) fluorescence at the neurite (Fig. 2,

[1]Division of Neurobiology, Department of Molecular and Cell Biology, Helen Wills Neuroscience Institute, University of California, Berkeley, CA 94720, USA. [2]Department of Neuroscience and Brain Technologies, Italian Institute of Technology, Via Morego 30, Genoa 16163, Italy.

*These authors contributed equally to this work.
†Present address: Department of Materials Science and Engineering, Geballe Laboratory for Advanced Materials, Stanford University, Stanford, CA 94305, USA.
‡To whom correspondence should be addressed. E-mail: mpoo@uclink.berkeley.edu

A, B, D, E, and G). In contrast, the same treatment induced a reduction of cGMP in cells expressing cGES-DE5 (Fig. 2, C, F and G). Conversely, the membrane-permeant cGMP analog 8-pCPT-cGMP (20 μM) or the nitric oxide donor (DEA NONOate, 200 μM), which is known to activate sGC, increased cGMP (Fig. 2, C, F and G) and reduced cAMP and PKA activity (Fig. 2, B, D, E and G).

The reciprocal regulation was also observed when the basal level of either cAMP or cGMP was modulated by altering its synthesis or degradation. Bath application of the AC inhibitor SQ-22536 (10 μM) resulted in not only the expected reduction of cAMP and PKA activity, but also in cGMP elevation (Fig. 2G). Treatment with the sGC inhibitor ODQ (1 μM) yielded opposite effects: reduction of cGMP and elevation of cAMP and PKA activity (Fig. 2G). Furthermore, the nonspecific phosphodiesterase (PDE) inhibitor 3-isobutyl-1-methylxanthine (IBMX, 50 μM) elevated both the basal cAMP/PKA and cGMP levels, whereas the cAMP-specific PDE4 inhibitor rolipram (1 μM) caused an expected increased cAMP/PKA level and a slight cGMP reduction (Fig. 2G). A peptide-based assay also confirmed that IBMX could elevate PKA activity in hippocampal cultures (fig. S3Cb), and that rolipram treatment or transfection with PDE4D small interfering RNAs (siRNAs) caused similar PKA elevation in cultured HEK-293T cells (fig. S1A). Thus, reciprocal regulation between cAMP and cGMP is constitutively present in these developing neurons, allowing adjustment of the basal level of these cyclic nucleotides bi-directionally. The antagonistic actions of cAMP/cGMP on axon/dendrite differentiation described above (Fig. 1) could be attributed directly to the reciprocal regulation between these two cyclic nucleotides.

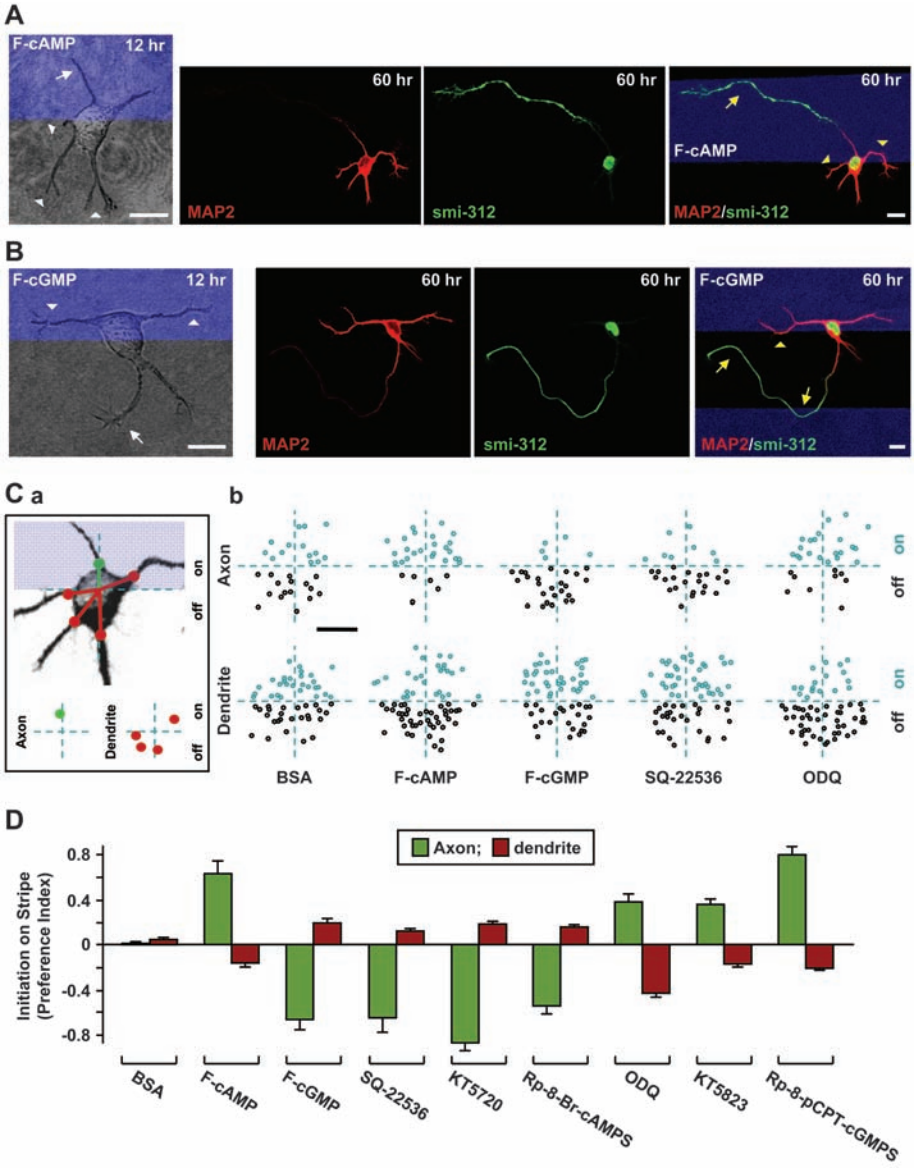

Fig. 1. Antagonistic effects of cAMP and cGMP on axon/dendrite initiation. (**A** and **B**) Images of cultured hippocampal neurons on substrates coated with stripes (blue) of F-cAMP or F-cGMP at 12 and 60 hours after cell plating and immunostained (at 60 hours) for axons and dendrites with smi-312 and MAP2 antibodies, respectively. White arrows and arrowheads: neurites that later became axons and dendrites, respectively. Yellow symbols: axon/dendrite turning at stripe boundary. Scale bars, 10 μm. (**C**) Preferential axon/dendrite initiation. (a) Diagram depicting the distribution of axon/dendrite initiation site (circles) relative to the center of the stripe boundary intersecting the soma. (b) Distribution of initiation sites on-stripe (blue) or off-stripe (black), for axons (30 cells) and all dendrites (10 cells) initiated on various striped substrates. Scale bar, 5 μm. (**D**) Preferential index for axon/dendrite initiation, shown as average ± SD [n = 3 to 5 cultures, 150 to 200 cells each, $P < 0.001$, two-tailed t test or Kolmogorov-Smirnov test, compared to bovine serum albumin (BSA)].

Mechanisms underlying reciprocal regulation. In various non-neuronal systems, cGMP-induced activation of PDEs inhibits cAMP signaling by increasing cAMP hydrolysis (*29*, *33*). Measurements with FRET reporters in cultured neurons showed that, after pre-incubation with IBMX, subsequent addition of NO-donor (or 8-pCPT-cGMP) and forskolin failed to induce reciprocal down-regulation of cAMP/PKA activity (Fig. 3, Aa and Ab) and cGMP (Fig. 3Ac), respectively, demonstrating the involvement of PDEs in this reciprocal regulation. Pre-incubation with rolipram, which by itself elevated the basal level of cAMP/PKA activity (Fig. 2G), abolished the 8-pCPT-cGMP–induced reduction of the PKA activity (Fig. 3Ad). The rolipram effect was specific, because the PDE2-specific inhibitor BAY 60-7550 had no effect (Fig. 3Ae), and it was not attributable to saturated cAMP elevation caused by rolipram, because further cAMP elevation could be achieved by adding forskolin to rolipram-treated cells (Fig. 3Af). Similarly, for the crosstalk from cAMP to cGMP, the forskolin-induced cGMP reduction could be abolished by the PDE3 inhibitor cilostamide (300 nM) (Fig. 3Ag) and was significantly diminished by the inhibitor of cGMP-specific PDE5 MY-5445 (30 μM) (Fig. 3Ah). Furthermore, although an NO donor greatly reduced the forskolin-induced PKA activity (Fig. 3Ba), it had no significant effect on the PKA activity induced by the nonhydrolyzable cAMP analog Sp-8-Br-cAMPS (Fig. 3Bb). Similarly, forskolin suppressed NO donor–induced cGMP elevation (Fig. 3Bc) but had no significant effect on the cGMP signal induced by the nonhydrolyzable cGMP analog 8-pCPT-cGMP (Fig. 3Bd).

In non-neuronal systems (*29*, *33*), PDE activities can be modulated by PKA/PKG-dependent phosphorylation. We found that forskolin-induced cGMP reduction was prevented by KT5720 (200 nM, Fig. 3Ai), and the reduction of PKA activity that was caused by 8-pCPT-cGMP was prevented by the PKG inhibitor KT5823 (200 nM, Fig. 3Aj). Thus, whereas reciprocal regulation between cAMP and cGMP is modulated by specific PDEs, PKA/PKG activation might

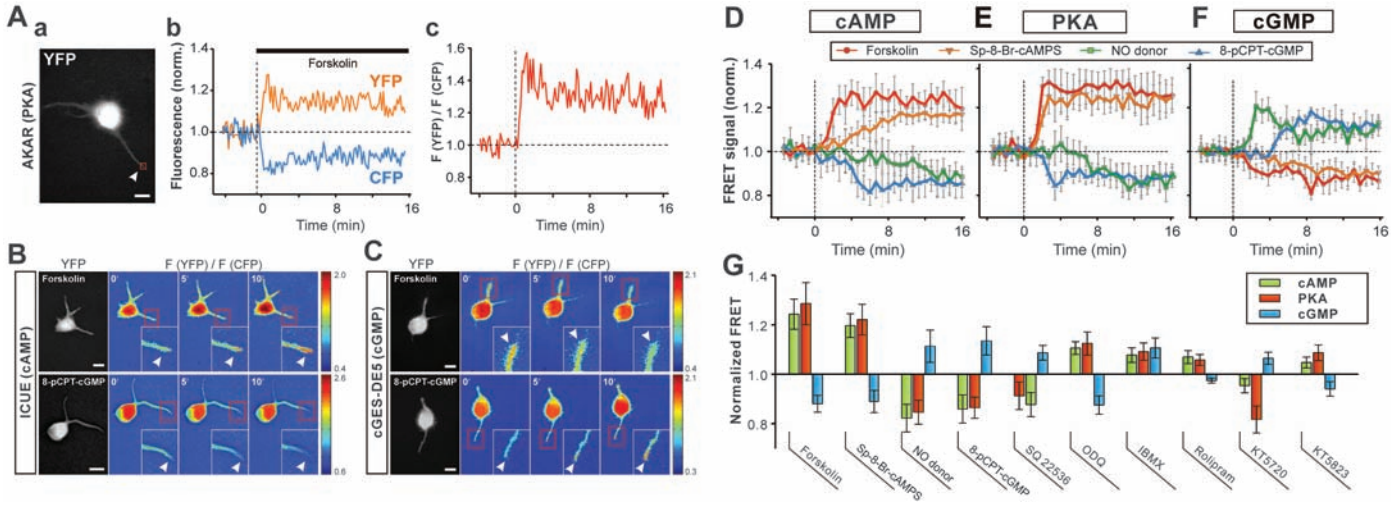

Fig. 2. Reciprocal regulation between cAMP and cGMP revealed by FRET imaging. (**A**) Forskolin-induced FRET signal for PKA activity. (a) YFP image of a hippocampal neuron expressing AKAR at 16 hours. Scale bar, 10 μm. (b) Forskolin-induced changes in YFP and CFP fluorescence at a neurite tip (red square in a), normalized by the average value before forskolin application. (c) Ratio of normalized YFP fluorescence [F(YFP)] to CFP fluorescence [F(CFP)], representing the FRET signal. (**B** and **C**) FRET signals observed at the neurite tip of 16-hours neurons expressing ICUE or cGES-DE5. The black and white images show YFP fluorescence and the color show FRET signals at different times (in min) after forskolin or 8-pCPT-cGMP application, coded in pseudocolors (scale bar on the right). Inset: Higher magnification images of FRET signals at the neurite tip. Scale bar, 10 μm. (**D** to **F**) FRET signal (at neurite tips) for all neurons expressing the ICUE [(D), cAMP], AKAR [(E), PKA] or cGES-DE5 [(F), cGMP], induced by the compound as indicated, averaged over 40-s bins and normalized by the mean control value before drug application (±SEM, n = 5 to 8 cells each, 1 or 2 per cell). (**G**) Reciprocal regulation between cAMP and cGMP and the role of PDEs and PKA/PKG. Data represent average FRET signals similar to that in (D) to (F) for cAMP, PKA, or cGMP at 10 to 20 min after drug application. Error bars indicate ±SEM, n = 5 to 8 cells each, 1 or 2 per cell.

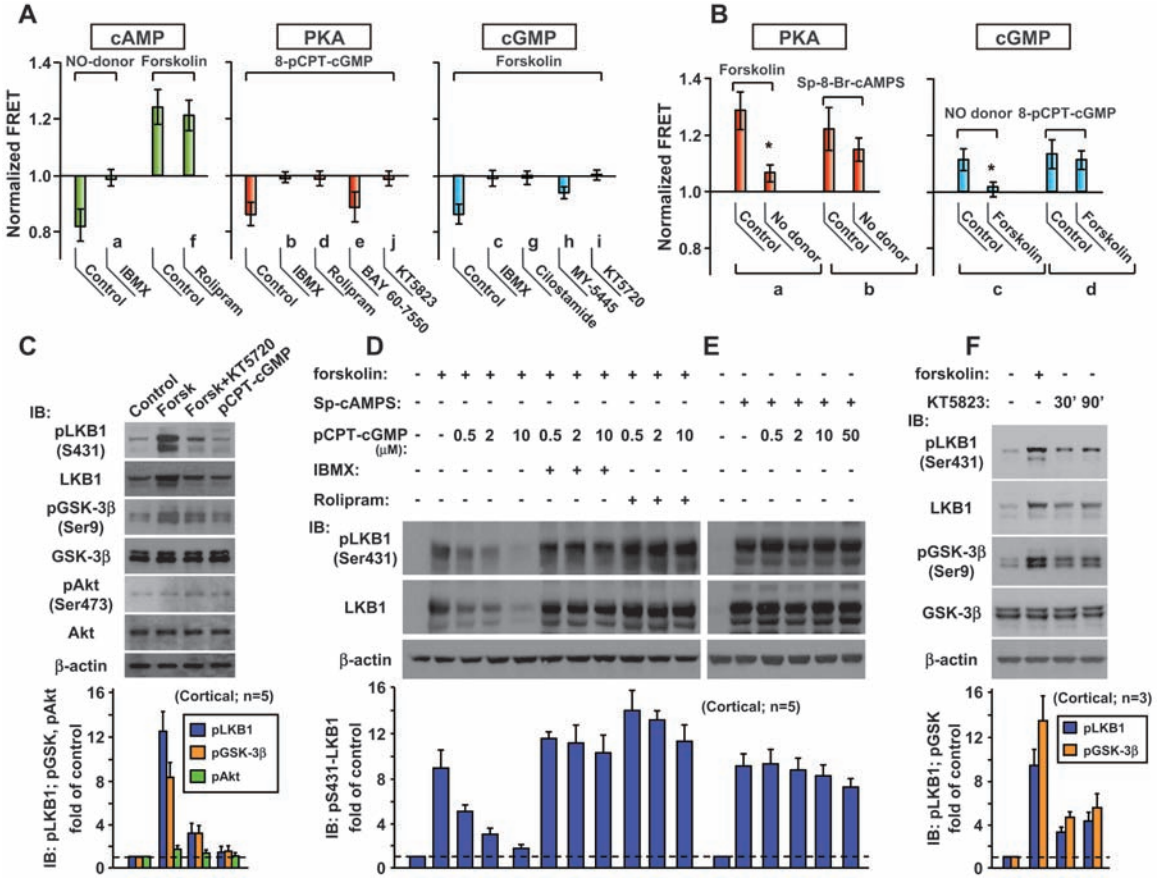

Fig. 3. The role of PDEs and PKA/PKG in reciprocal cAMP/cGMP regulation and phosphorylation of axon determinants LKB1 and GSK-3β. (**A** and **B**) Average FRET signals for cAMP, PKA, and cGMP at 10 to 20 min after bath application of the compound indicated above, in the presence of the drug indicated below (±SEM, 5 to 8 cells each, 1 or 2 per cell). In (A) and (B), data significantly different from control are marked by an asterisk ($P < 0.05$, Mann-Whitney U test). (**C**) Immunoblot analysis of cAMP-induced phosphorylation of LKB1, GSK-3β, and Akt on total cell lysates of 5-day cultures of cortical neurons, using antibodies specific to the phosphorylation site or the protein. Forsk., forskolin. Histograms show the average phosphorylation level (±SD, n = 5), normalized to β-actin and shown as fold of control. (**D** and **E**) Antagonistic action of cGMP activity on cAMP-induced LKB1 phosphorylation is mediated by cAMP-specific PDEs. Immunoblot analysis as in (C). Cells were treated with forskolin (D) or Sp-8-Br-cAMPS (E), either alone or in combination with increasing concentrations of 8-pCPT-cGMP, and in the absence or presence of IBMX or rolipram. (**F**) Inhibition of PKG by KT5823 resulted in LKB1 and GSK-3β phosphorylation. Immunoblot analysis was as in (C).

also regulate AC/sGC or selective PDEs (*29*, *33*). This hypothesis is supported by the finding that KT5720 alone not only reduced the PKA activity, but also increased cGMP and reduced cAMP, whereas KT5823 alone elevated cAMP/PKA and reduced cGMP (Fig. 2G).

cGMP antagonizes the phosphorylation of axon determinants. To further explore the mechanisms underlying the antagonistic actions of cAMP and cGMP on axon initiation, we inquired whether this antagonism is reflected in the phosphorylation of LKB1 (*12*), GSK-3β (*8*, *16*), and Akt (*8*, *15*), which are proteins that promote axon formation after their phosphorylation. Immunoblotting of lysates of cultured cortical neurons using phosphorylation site–specific antibodies showed that elevating cAMP synthesis with forskolin caused a PKA-dependent increase of LKB1 phosphorylation at serine 431 (S431) and of GSK-3β at S9 (Fig. 3C), and this effect correlated with the increased level of total LKB1 (*12*). Furthermore, when cultures that were plated on F-cAMP stripe were transfected with siRNA to LKB1 (*12*) and examined at 60 hours, the polarized population of these transfected neurons showed reduction in preferential axon initiation at the stripe boundary (fig. S2A). Forskolin caused no detectable Akt phosphorylation at S473 (Fig. 3C). Conversely, elevating cGMP by bath application of 8-pCPT-cGMP did not cause detectable reduction of LKB1 and GSK-3β phosphorylation (Fig. 3C), probably because of the low resolution of the immunoblotting method. However, in HEK-293T cells expressing an LKB1 construct, 8-pCPT-cGMP markedly reduced LKB1 phosphorylation and the total amount of LKB1 (fig. S2B). Activation of PKA activity by forskolin was confirmed in hippocampal cultures by a peptide-based assay (fig. S3, A and Ca), which also showed a dose-dependent reduction of the basal PKA activity in these cultured neurons by 8-pCPT-cGMP treatment (fig. S3B). The 8-pCPT-cGMP effects on the phosphorylation and stability of LKB1 depended on the PKA site 431, because they were absent in HEK-293T cells expressing LKB1 with a serine-to-alanine mutation (*12*) at this site (fig. S2B).

We further examined the mechanism underlying the effect of cGMP on PKA-dependent LKB1 phosphorylation. Bath-applied 8-pCPT-cGMP dose-dependently reduced the phosphorylation (at S431) and stabilization of LKB1 induced by forskolin in cultured cortical neurons (Fig. 3D). This antagonistic cGMP effect was abolished by either IBMX or rolipram (Fig. 3D), indicating that cGMP reduced the cAMP level primarily by PDE4 activation. The antagonistic effect of 8-pCPT-cGMP on LKB1 phosphorylation was largely absent when PDE-resistant Sp-8-Br-cAMPS was used instead of forskolin (Fig. 3E). The peptide-based PKA assay also confirmed these findings in cultured hippocampal neurons (fig. S3). Treatment with KT5823 resulted in a slight elevation of PKA activity in hippocampal neurons (fig. S3Cb) and LKB1 phosphorylation/stabilization in cortical cultures (Fig. 3F), consistent with the FRET imaging result showing that PKA/PKG inhibition could modulate the cAMP/ cGMP level (Fig. 2).

Perturbation of cAMP/cGMP affects neuronal polarization in vivo. We also investigated the role of cAMP/cGMP in the development of cortical neurons in vivo by elevating cAMP and reducing cGMP in newly generated cortical neurons in rat embryos. This was achieved by in utero electroporation (*34*) of constructs expressing enhanced green fluorescent protein (EGFP) and specific siRNAs against either cAMP-selective phosphodiesterase 4D (PDE4D) (*12*) or soluble guanylate

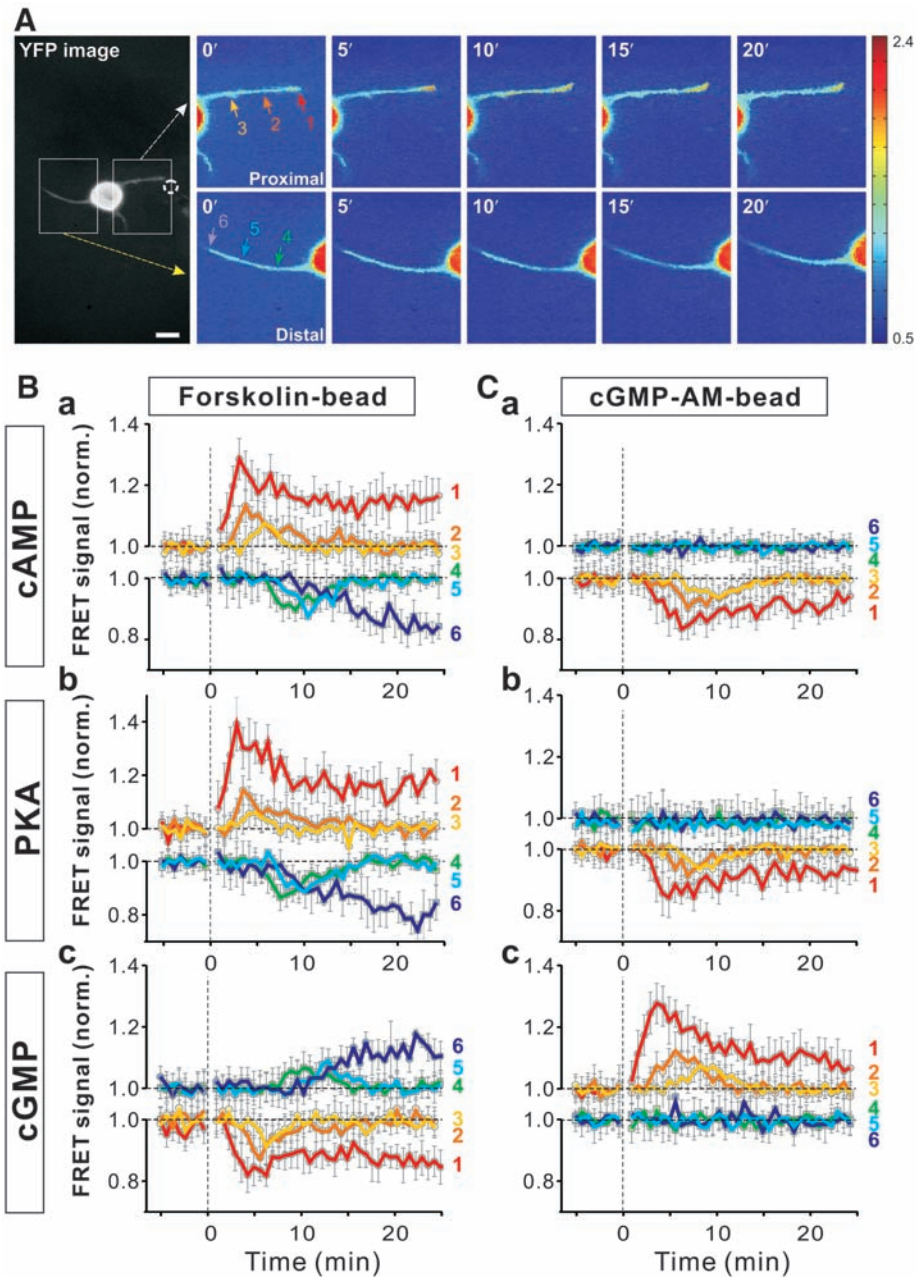

Fig. 4. Local cAMP elevation induced long-range cAMP reduction, but local cGMP elevation had no long-range effect. (**A**) YFP fluorescence and FRET signals for cAMP in an ICUE-expressing hippocampal neuron at 16 hours, at different times (in minutes) after the contact by a forskolin-coated glass bead (dashed circle) in the bead-contacted (upper panels) and noncontacted (lower panels) neurite. Scale bar, 10 μm. (**B**) Average FRET signals for cAMP, PKA, or cGMP in cells expressing ICUE (a), AKAR (b), or cGES-DES (c), respectively, detected at different locations along the forskolin bead–contacted neurite (1 to 3) and all other neurites (4 to 6). For bead-contacted neurites, the signals were measured at the bead contact site at the tip (1) and at sites 1/3 (2) and 2/3 (3) neurite lengths from the tip [see illustration in (A)]. For all other neurites, the signals were measured at sites 1/3 (4) or 2/3 (5) of neurite length from the soma, and at the tip of the neurite (6). Data represent average ± SEM (n = 5 to 10 cells, including all neurites). (**C**) Same as in (B), except that the bead was coated with cGMP-AM.

cyclase-β1 subunit (sGC-β1) (fig. S1B) into a subpopulation of neural progenitor cells at embryonic day 18 (E18). We found that cortical neurons expressing the siRNA against either PDE4D or sGC-β1 exhibited impaired radial migration to the cortical plate (CP) in E21 embryos (fig. S4, A to C). Whereas most neurons had a single-neurite (unipolar) or two-neurite (bipolar) morphology in control E21 rat embryos, a large percentage of PDE4D or sGC-β1 siRNA-expressing neurons were multipolar (fig. S4, D and E). The polarization defects correlated positively with the level of siRNA expression (fig. S4, F to H). Similar polarization and migration defects were also observed for PDE4D or sGC-β1 siRNA-expressing neurons in postnatal day 0 (P0) rat cortices (fig. S5). Thus, elevating cAMP and reducing cGMP produced similar defects in developing cortical neurons in vivo. However, whether there is a causal relationship between the tightly linked processes of neuronal polarization and radial migration during this stage of development and whether cAMP/cGMP signaling is involved in both processes remain to be further elucidated.

Local cAMP elevation causes long-range cAMP suppression. The reciprocal regulation between cAMP and cGMP could facilitate neurite differentiation along the axonal and dendritic route when cAMP and cGMP are locally elevated, respectively. To examine how this local cAMP/cGMP elevation affects the global cAMP/cGMP signaling of the entire neuron, we manipulated a glass bead coated with forskolin (SOM text) into contact with an undifferentiated neurite of hippocampal neurons expressing the FRET reporter for cAMP or PKA activity. We found a marked and persistent increase in cAMP or PKA signals at the bead contact site (Fig. 4, A, Ba, and Bb, and fig. S6) and transient cAMP/PKA signals along the shaft of bead-contacted neurites, with decreasing amplitude and longer delay of onset at more proximal locations toward the soma (Fig. 4, A, Ba, and Bb, and fig. S6). The apparent spread of cAMP/PKA activity along the neurite was not caused by the diffusion of forskolin extracellularly, because no signal was observed when the forskolin-coated bead was placed in close proximity (<2 μm) but not in direct contact with the neurite (fig. S6). After the forskolin-bead contact, we observed a striking reduction of cAMP/PKA signals in all other neurites (Fig. 4, A, Ba, and Bb, and fig. S6), with increasing extent of reduction and a longer delay of onset at more distal locations. In a reciprocal manner, in cells expressing the cGMP reporter cGES-DE5, the cGMP signal was reduced at the forskolin bead-contacted neurite but increased in all other neurites, with a pattern exactly mirroring that of cAMP/PKA (Fig. 4Bc).

When similar experiments were done using a glass bead coated with the membrane-permeable cGMP-AM (acetoxymethyl ester), we found a local elevation of the cGMP signal and a reduction of the cAMP/PKA signal at the bead-contacted neurite, but a complete absence of any long-range effect on either cGMP or cAMP/PKA in all other neurites (Fig. 4C and fig. S6). Because the cGMP-AM bead also induced a local cAMP/PKA reduction, the lack of effect in other neurites indicates that the long-range cAMP signaling is unidirectional, triggered only by cAMP elevation. The existence of long-range self–down-regulation of cAMP but not cGMP immediately suggests a mechanism for the formation of one axon and multiple dendrites: Axon induction by local cAMP elevation leads to suppression of axon formation and promotion of dendrite formation at all other neurites, whereas dendrite induction by local cGMP elevation has no long-range effect.

Differential growth regulation by cAMP and cGMP. Polarization of cultured hippocampal neurons begins with growth acceleration of a single undifferentiated neurite (*1*, *2*, *4*, *21*), suggesting that axon initiation may be achieved by signals acting directly on specific cytoskeletal components (*35*–*37*) that accelerate neurite growth. Differential growth regulation may contribute to the antagonistic action by cAMP and cGMP on axon/dendrite differentiation. We thus examined the effect of global manipulation of cAMP/cGMP activities on the growth of undifferentiated neurites and axons/dendrites. Bath application of various pharmacological agents at 2 hours after cell plating and neurite length measurements at 9 hours showed that global cAMP elevation (with forskolin) or cGMP reduction (with ODQ) enhanced the growth primarily of one or two neurites (Fig. 5A), whereas global cGMP elevation (with 8-pCPT-cGMP) or cAMP reduction (with SQ-22536) resulted in relatively uniform growth promotion of all neurites (Fig. 5A). The asymmetry in neurite growth promotion by cAMP elevation may reflect the dominance of a single neurite that first acquired the highest cAMP elevation, together with long-range self–down-regulation of cAMP that suppressed the growth of most other neurites. By 48 hours after plating, global elevation of cAMP (or reduction of cGMP) increased the axon length but reduced the dendrite length, whereas global elevation of cGMP (or reduction of cAMP) had opposite effects (Fig. 5B), consistent with cAMP/cGMP antagonism. These results also suggest that axon and dendrite growth involve cAMP- and cGMP-dependent activation of specific cellular components, respectively.

Discussion. Many extracellular factors known to regulate neuron polarization, including brain-derived neurotrophic factor (BDNF) (*8*, *12*), nerve growth factor (NGF) (*9*), Sema3A (*38*), netrin-1

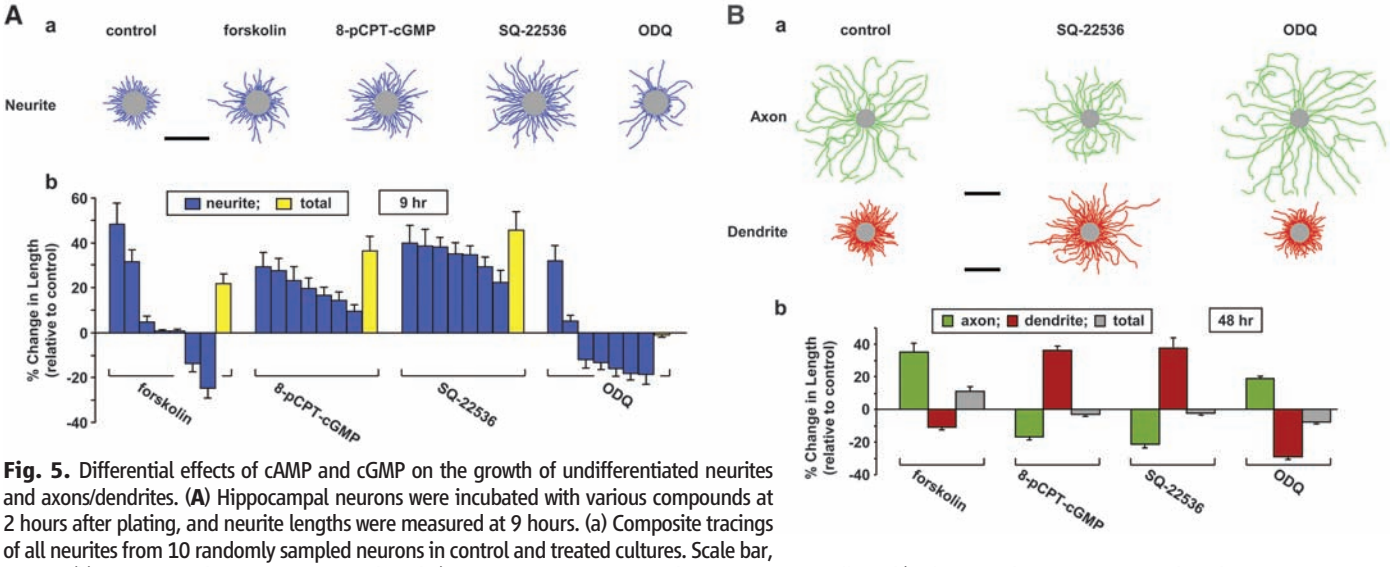

Fig. 5. Differential effects of cAMP and cGMP on the growth of undifferentiated neurites and axons/dendrites. (**A**) Hippocampal neurons were incubated with various compounds at 2 hours after plating, and neurite lengths were measured at 9 hours. (a) Composite tracings of all neurites from 10 randomly sampled neurons in control and treated cultures. Scale bar, 50 μm. (b) Percentage difference in neurite length (average ± SD; n = 3 to 5 cultures, 70 to 100 cells each) relative to the average neurite length for 100 neurons in parallel control cultures, for up to the first seven longest neurites (blue) and for all neurites (yellow). (**B**) Axon and dendrite lengths at 60 hours (compound added at 2 hours), determined by immunostaining with axon- and dendrite-specific markers, smi-312 and MAP2, respectively. (a) Composites of tracings of randomly sampled cells (axons, 25 cells, green; dendrites, 15 cells, red) in control and treated cultures. Scale bar, 100 (axons) and 50 (dendrites) μm. (b) Percentage difference of axon and dendrite lengths (average ± SD; n = 3 to 5 cultures, 70 to 100 cells each) relative to those in 100 control neurons in parallel cultures.

(*10*), Wnt (*11*), and laminin (*6*, *7*), could modulate the cAMP or cGMP level in neurons (*12*, *38*–*43*). Localized exposure to one or more of such factors may create a cytoplasmic asymmetry for axon/dendrite initiation. Perturbation of the cAMP/cGMP level resulted in neuronal polarization defects in the developing cortex (figs. S4 and S5), but the cAMP/cGMP-modulating extracellular factors that are responsible for polarizing the neurons in vivo remain to be identified. In a model for distinct actions of local versus global cAMP/cGMP signaling (fig. S7), we propose that axons and dendrites are induced via localized cAMP and cGMP signals, and local antagonistic interactions between cAMP and cGMP pathways ensure that axon initiation is accompanied by the inhibition of dendrite formation, and vice versa. The cAMP signal acts through phosphorylated LKB1 (*12*) and GSK-3β (*8*, *16*) and their downstream effectors, which may converge with the PI3K pathway at several levels to promote axon initiation (*15*, *19*, *44*–*46*), whereas the cGMP signal suppresses axon formation via reciprocal down-regulation of cAMP/PKA-dependent phosphorylation of LKB1 and GSK-3β (Fig. 3), as well as specifically promotes dendrite growth (Fig. 5) via cellular processes yet to be identified (fig. S7).

Long-range inhibitory signaling in neurons has been reported. Local contact of a neurite with a target cell (*47*) or laminin-coated surface (*6*, *7*), or local perfusion of a neurite with forskolin (*48*), all led to growth inhibition of distant neurites. This inhibitory effect may be caused by the long-range self-suppression of cAMP, although the mechanism underlying this long-range cAMP self-antagonism remains to be elucidated. The absence of long-range signaling resulting from local cGMP elevation suggests the framework of axon dominance signaling in the coordinated axon/dendrite differentiation; whereas local cAMP/cGMP reciprocal regulation helps to channel the differentiation process along either an axonal or dendritic route, the long-range cAMP self-suppression ensures the formation of only one axon.

References and Notes

1. N. Arimura, K. Kaibuchi, *Nat. Rev. Neurosci.* **8**, 194 (2007).
2. A. P. Barnes, D. Solecki, F. Polleux, *Curr. Opin. Neurobiol.* **18**, 44 (2008).
3. F. C. de Anda *et al.*, *Nature* **436**, 704 (2005).
4. K. Goslin, G. Banker, *J. Cell Biol.* **108**, 1507 (1989).
5. C. Jacobson, B. Schnapp, G. A. Banker, *Neuron* **49**, 797 (2006).
6. T. Esch, V. Lemmon, G. Banker, *J. Neurosci.* **19**, 6417 (1999).
7. C. Ménager, N. Arimura, Y. Fukata, K. Kaibuchi, *J. Neurochem.* **89**, 109 (2004).
8. T. Yoshimura *et al.*, *Cell* **120**, 137 (2005).
9. J. S. Da Silva, T. Hasegawa, T. Miyagi, C. G. Dotti, J. Abad-Rodriguez, *Nat. Neurosci.* **8**, 606 (2005).
10. C. E. Adler, R. D. Fetter, C. I. Bargmann, *Nat. Neurosci.* **9**, 511 (2006).
11. M. A. Hilliard, C. I. Bargmann, *Dev. Cell* **10**, 379 (2006).
12. M. Shelly, L. Cancedda, S. Heilshorn, G. Sumbre, M. M. Poo, *Cell* **129**, 565 (2007).
13. M. Fivaz, S. Bandara, T. Inoue, T. Meyer, *Curr. Biol.* **18**, 44 (2008).
14. M. Toriyama *et al.*, *J. Cell Biol.* **175**, 147 (2006).
15. S. H. Shi, L. Y. Jan, Y. N. Jan, *Cell* **112**, 63 (2003).
16. H. Jiang, W. Guo, X. Liang, Y. Rao, *Cell* **120**, 123 (2005).
17. J. C. Schwamborn, A. W. Püschel, *Nat. Neurosci.* **7**, 923 (2004).
18. M. Kishi, Y. A. Pan, J. G. Crump, J. R. Sanes, *Science* **307**, 929 (2005).
19. A. P. Barnes *et al.*, *Cell* **129**, 549 (2007).
20. C. G. Dotti, C. A. Sullivan, G. A. Banker, *J. Neurosci.* **8**, 1454 (1988).
21. A. M. Craig, G. Banker, *Annu. Rev. Neurosci.* **17**, 267 (1994).
22. A. M. Lohof, M. Quillan, Y. Dan, M. M. Poo, *J. Neurosci.* **12**, 1253 (1992).
23. M. Nishiyama *et al.*, *Nature* **423**, 990 (2003).
24. N. Buttner, S. A. Siegelbaum, *J. Neurophysiol.* **90**, 586 (2003).
25. H. C. Hartzell, R. Fischmeister, *Nature* **323**, 273 (1986).
26. A. Hempel, T. Noll, A. Muhs, H. M. Piper, *Am. J. Physiol.* **270**, H1264 (1996).
27. C. Peña-Rasgado, V. A. Kimler, K. D. McGruder, J. Tie, H. Rasgado-Flores, *Am. J. Physiol.* **267**, C1319 (1994).
28. N. D. Goldberg *et al.*, *Adv. Cyclic Nucleotide Res.* **5**, 307 (1975).
29. M. Zaccolo, M. A. Movsesian, *Circ. Res.* **100**, 1569 (2007).
30. L. M. DiPilato, X. Cheng, J. Zhang, *Proc. Natl. Acad. Sci. U.S.A.* **101**, 16513 (2004).
31. V. O. Nikolaev, S. Gambaryan, M. J. Lohse, *Nat. Methods* **3**, 23 (2006).
32. J. Zhang, Y. Ma, S. S. Taylor, R. Y. Tsien, *Proc. Natl. Acad. Sci. U.S.A.* **98**, 14997 (2001).
33. F. S. Menniti, W. S. Faraci, C. J. Schmidt, *Nat. Rev. Drug Discov.* **5**, 660 (2006).
34. T. Saito, N. Nakatsuji, *Dev. Biol.* **240**, 237 (2001).
35. F. Bradke, C. G. Dotti, *Science* **283**, 1931 (1999).
36. H. Witte, D. Neukirchen, F. Bradke, *J. Cell Biol.* **180**, 619 (2008).
37. H. Witte, F. Bradke, *Curr. Opin. Neurobiol.* **18**, 479 (2008).
38. F. Polleux, T. Morrow, A. Ghosh, *Nature* **404**, 567 (2000).
39. H. J. Song, G. L. Ming, M. M. Poo, *Nature* **388**, 275 (1997).
40. G. L. Ming *et al.*, *Neuron* **19**, 1225 (1997).
41. Y. Gao, E. Nikulina, W. Mellado, M. T. Filbin, *J. Neurosci.* **23**, 11770 (2003).
42. K. Togashi *et al.*, *Neuron* **58**, 694 (2008).
43. V. H. Höpker, D. Shewan, M. Tessier-Lavigne, M. M. Poo, C. Holt, *Nature* **401**, 69 (1999).
44. O. Ossipova, N. Bardeesy, R. A. DePinho, J. B. A. Green, *Nat. Cell Biol.* **5**, 889 (2003).
45. Y. J. Choi *et al.*, *Genes Dev.* **22**, 2485 (2008).
46. J. Wildonger, L. Y. Jan, Y. N. Jan, *Genes Dev.* **22**, 2447 (2008).
47. D. J. Goldberg, S. Schacher, *Dev. Biol.* **124**, 35 (1987).
48. J. Q. Zheng, Z. Zheng, M. M. Poo, *J. Cell Biol.* **127**, 1693 (1994).

49. We thank R. Thakar, S. Li, M. Nasir, and D. Liepmann (University of California at Berkeley) for help with poly(dimethylsiloxane) microfluidic molds; J. Zhang (Johns Hopkins University) for the ICUE and AKAR FRET probes; M. J. Lohse (University of Wurzburg) for the cGES-DE5 FRET probe; M. Feller and S. Pautot (University of California at Berkeley) for advice on FRET imaging and bead coating; and M. Hung for help with culture preparations. This work was supported in part by a grant from the National Institutes of Health (NS-22764).

Supporting Online Material

www.sciencemag.org/cgi/content/full/327/5965/547/DC1
Materials and Methods
SOM Text
Figs. S1 to S7

27 July 2009; accepted 10 December 2009
10.1126/science.1179735

REPORTS

Phase Transitions of Adsorbed Atoms on the Surface of a Carbon Nanotube

Zenghui Wang, Jiang Wei, Peter Morse, J. Gregory Dash, Oscar E. Vilches, David H. Cobden*

Phase transitions of adsorbed atoms and molecules on two-dimensional substrates are well explored, but similar transitions in the one-dimensional limit have been more difficult to study experimentally. Suspended carbon nanotubes can act as nanoscale resonators with remarkable electromechanical properties and the ability to detect adsorption at the level of single atoms. We used single-walled carbon nanotube resonators to study the phase behavior of adsorbed argon and krypton atoms as well as their coupling to the substrate electrons. By monitoring the resonance frequency in the presence of gases, we observed the formation of monolayers on the cylindrical surface, phase transitions within them, and simultaneous modification of the electrical conductance.

Films of atoms or molecules adsorbed on surfaces exhibit many kinds of ordering that reflect interactions between the adsorbates as well as with the surface. One of the simplest model systems, rare gases on bulk exfoliated graphite, exhibits a huge range of two-dimensional (2D) phenomena within the first adsorbed layer, including 2D melting, transitions between solids that are either commensurate or incommensurate with the graphene lattice, and critical behavior (*1*, *2*). Here, we explore the phase behavior of argon and krypton on carbon nanotubes, where the dimensionality of the substrate approaches the 1D limit, and report effects on the electronic conductance that reflect adsorbate-substrate interactions. We map out this phase behavior using nanomechanical resonators based on individual suspended single-walled nanotubes (SWNTs) (*3*–*6*). This platform combines remarkable electrical (*7*–*9*) and electromechanical (*10*–*12*) properties with extreme mass sensitivity (*13*–*15*) and allows simultaneous measurement of both the precise amount of adsorbed substance and its effect on the electrical

Department of Physics, University of Washington, Seattle, WA 98195–1560, USA.

*To whom correspondence should be addressed. E-mail: cobden@u.washington.edu